ΔΛ-Isomerism of Mixed 1,3-Diketonate Complexes of Ru(III)−A Designed New Source of Chirality in Nematic Liquid Crystals†

Yuki Matsuoka,‡ Hisako Sato,‡,§ Akihiko Yamagishi,‡,§ Kentaro Okamoto,|| and Naomi Hoshino*,⊥

Department of Earth and Planetary Science, Graduate School of Science, The University of Tokyo, Tokyo 113-0033, Japan, CREST, Japan Science and Technology Agency, 4-1-8 Honcho, Kawaguchi, Saitama 332-0012, Japan, Opto-Single-Crystal Group, Advanced Materials Laboratory, National Institute for Material Science, 1-1 Namiki, Tsukuba, Ibaraki 305-0044, Japan, and Division of Chemistry, Graduate School of Science, Hokkaido University, Sapporo 060-0810, Japan

Received October 27, 2004. Revised Manuscript Received July 9, 2005

A high-power chiral dopant system involving 6-coordinate metal complexes was designed on the basis of a shape model. Accordingly, a series of mixed 1,3-diketonate complexes of Ru(III), [Ru(acac)$_2$(L-*n*)], in which acac = acetylacetonate and L-*n* = dibenzoylmethanate substituted with *n* octyloxy groups (abbreviated as **Ru-*n*** hereafter), was prepared and optically resolved. Their performance as chiral dopants was evaluated in terms of helical twisting power (HTP) in a room-temperature nematic liquid crystal, *N*-(4-methoxybenzylidene)-4-*n*-butylaniline (MBBA), by measuring the helical pitch lengths and CD spectra for the induced chiral nematic phases. The Δ- and Λ-enantiomers induced macroscopic left-handed (*M*) and right-handed (*P*) helices, respectively, and the (absolute) values for HTP have proven to be remarkably large, e.g. $\beta_M = 1.8 \times 10^2\ \mu m^{-1}$ in the case of Λ-**Ru-2**. The induced CD spectra for the dilute MBBA* materials (the asterisk denotes in this paper that MBBA has been doped with a chiral substance) were fit to the interpretation that persistent helical alignment of host molecules was generated. We also performed quantum chemical calculations for the optimum configuration of model Al(III) complexes with and without MBBA molecules and found that two liquid crystal molecules will eventually form a negative dihedral angle (left-handed twist) over the Δ-enantiomer of dialkylated complex.

Introduction

The effect of chirality in liquid crystals has long intrigued scientists in broad disciplines[1,2] since the discovery of a cholesteric liquid crystal in 1888, and it continues to be so as bent-core mesogens have added complexity to the issue lately. As to how the polar ordering is associated with symmetry, some workers favor a view that molecules of C_{2v} symmetry can still give rise to layer chirality,[3] if coupled to the tilt, while others seem to believe in molecular conformational chirality stabilized in the mesophase.[4] It is worthwhile to look at the phase chirality in these new lights and to reconsider how the presence of chiral center(s) as an *explicitly* symmetry-breaking element aids in unveiling interesting properties of anisotropic molecular fluids.

The phenomenon of chiral phase induction has been actively investigated also in the areas of organic[5] and polymer[6] chemistries and is recognized as a useful means of stereochemistry research nowadays.[7] The nematic liquid crystal turns into a chiral nematic by doping with a chiral substance and forms a helical superstructure, the pitch (*p*) of which characterizes the helical twisting power (HTP) of the dopant. The molecular HTP (β_M) of a pure enantiomer can be defined by eq 1

$$\beta_M = \left(\frac{\partial p^{-1}}{\partial x}\right)_{x\to 0} \quad (1)$$

where *x* denotes mole fraction of the enatiomer, and positive and negative values of β_M correspond to induced right-handed (*P*) and left-handed (*M*) helices, respectively.

* Corresponding author. E-mail: hoshino@sci.hokudai.ac.jp.

† A part of this work was presented at the 8th International Symposium on Metallomesogens (ISM2003), Namur, Belgium, May 28−31, 2003.

‡ The University of Tokyo.

§ CREST, JST.

|| National Institute for Material Science.

⊥ Hokkaido University.

(1) *Chirality in Liquid Crystals*; Kitzerow, H.-S., Bahr, C., Eds.; Springer-Verlag: New York, 2001.

(2) (a) Solladié, G.; Zimmermann, R. G. *Angew. Chem., Int. Ed. Engl.* **1984**, *23*, 348−362. (b) Goodby, J. W. *J. Mater. Chem.* **1991**, *1*, 307−318. (c) Goodby, J. W.; Slaney, A. J.; Booth, C. J.; Nishiyama, I.; Vuijk, J. D.; Styring, P.; Toyne, K. J. *Mol. Cryst. Liq. Cryst.* **1994**, *243*, 231−298. (d) Lubensky, T. C.; Harris, A. B.; Kamien, R. D.; Yan, G. *Ferroelectrics* **1998**, *212*, 1−20.

(3) (a) Link, D. R.; Natale, G.; Shao, R.; Maclennan, J. E.; Clark, N. A.; Körblova, E.; Walba, D. M. *Science* **1997**, *278*, 1924−1927. (b) Coleman, D. R.; Fernsler, J.; Chattham, N.; Nakata, M.; Takanishi, Y.; Körblova, E.; Link, D. R.; Shao, R.-F.; Jang, W. G.; Maclennan, J. E.; Mondainn-Monval, O.; Boyer, C.; Weissflog, W.; Pelzl, G.; Chien, L.-C.; Zasadzinski, J.; Watanabe, J.; Walba, D. M.; Takezoe, H.; Clark, N. A. *Science* **2003**, *301*, 1204−1211, and references therein.

(4) (a) Imase, T.; Kawauchi, S.; Watanabe, J. *J. Mol. Struct.* **2001**, *560*, 275−281. (b) Kajitani, T.; Masu, H.; Kohmoto, S.; Yamamoto, M.; Yamaguchi, K.; Kishikawa, K. *J. Am. Chem. Soc.* **2005**, *127*, 1124−1125.

(5) (a) Pieraccini, S.; Donnoli, M. I.; Ferrarini, A.; Gottarelli, G.; Licini, G.; Rosini, C.; Superchi, S.; Spada, G. P. *J. Org. Chem.* **2003**, *68*, 519−526. (b) Ferrarini, A.; Gottarelli, G.; Nordio, P. L.; Spada, G. P. *J. Chem. Soc., Perkin Trans. 2* **1999**, 411−417. (c) Gottarelli, G.; Hilbert, M.; Samori, B.; Solladié, G.; Spada, G. P.; Zimmermann, R. *J. Am. Chem. Soc.* **1983**, *105*, 7318−7321.

(6) Tang, K.; Green, M. M.; Cheon, K. S.; Selinger, J. V.; Garetz, B. A. *J. Am. Chem. Soc.* **2003**, *125*, 7313−7323.

(7) Eelkema, R.; van Delden, R. A.; Feringa, B. L. *Angew. Chem., Int. Ed.* **2004**, *43*, 5013−5016.

10.1021/cm048121b CCC: $30.25
Published on Web 09/13/2005

Chart 1. Structure of the Complexes Studied (Illustrated for the Δ-Enantiomers)

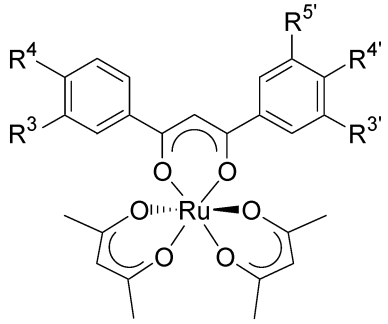

Δ-**Ru**-*n*

n = 0; $R^3=R^4=R^{3'}=R^{4'}=R^{5'}=H$

n = 2; $R^4=R^{4'}=OC_8H_{17}$: $R^3=R^{3'}=R^{5'}=H$

n = 3; $R^3=R^4=R^{4'}=OC_8H_{17}$: $R^{3'}=R^{5'}=H$

n = 4; $R^3=R^4=R^{3'}=R^{4'}=OC_8H_{17}$: $R^{5'}=H$

n = 5; $R^3=R^4=R^{3'}=R^{4'}=R^{5'}=OC_8H_{17}$

A critical question is how to correlate β_M to the dopant's chemical structure. The ΔΛ-isomerism of 6-coordinate tris-chelates of transition metals bears unique steric and electronic characteristics, not achievable by carbon centers, and they are expected to provide a significant new insight into the chirality recognition in liquid crystals. Spada and co-workers have demonstrated that enantiomerically pure metal acetylacetonates, [M(acac)$_3$], that belong to the D_3 point group have high ability to induce chiral nematic phases.[8] We also communicated that the Δ-enantiomer of the Ru(II) complex [Ru(acac)$_2$(obpy)] (obpy = 5,5′-(4-octylphenyloxycarbonyl)-2,2′-bipyridyl), designed to have C_2 symmetry with the (acac)$_2$ moiety acting as "chiral blades", has a remarkably high HTP for a nematic liquid crystal.[9,10] High-power chiral additives are potentially useful in unconventional LC applications, such as displays in the reflection mode or based on the electroclinic effect, not to mention the ferroelectric property. Our strategic design (for high HTP) for the metal complex dopants is given below.

The ligand design has been elaborated in the experimental work. To alleviate a potential problem of chemical instability and further improve the dopant performance, Ru(III) complexes were chosen for this study. The 4d metal complexes are generally resistant to thermal and/or photochemical racemization, although less expensive metal species such as Co(III) would be suited better to practical uses. Besides, synthetic procedures for mixed 1,3-diketonate complexes of desired composition are known for Ru(III). The 1,3-diketones not only furnish anionic ligands but also are synthetically more versatile and facilitate investigations of structure−performance relations. Thus, a new series of Ru(III) complexes, [Ru(acac)$_2$(L-*n*)] (L-*n* = a dibenzoylmethanate ligand substituted with *n* octyloxy chains) (**Ru-*n***, Chart 1), were prepared, and the number of octyloxy groups (*n*) was varied from 0 (unsubstituted) to 2 through 5. They were optically resolved into pure enantiomers by means of clay column chromatography, and their HTP values were determined. MBBA [*N*-(4-methoxybenzylidene)-4-*n*-butylaniline], an ambient-temperature nematic host, provides a clue for the handedness of helical superstructure induced by the chiral doping. The induced CD (ICD) spectra were measured for MBBA* materials obtained by doping with either Δ- or Λ-**Ru-*n*** under various concentrations, and the usefulness of the ICD spectroscopy will be highlighted. We also conducted ab initio calculations for the most stable geometry of an Al(III) analogue to our complex, **Al-2**, and of a trio of the complex and a pair of MBBA molecules, [Δ-**Al-2** + 2MBBA]. The computational information on the chirality recognition effect in the locus of chiral blades will be discussed.

Results and Discussion

Dopant Design Principle. We wish to explain first how we came to choose the ΔΛ-chirality, particularly of C_2 symmetry. It is based on the realization that the metal complexes of rigid, 6-coordinate (orthogonal) coordination geometry can most easily implement the features theoretically predicted to be effective. Ferrarini et al. reported a phenomenological approach[11] to the induced chiral nematic phases, and described the dopant's HTP by eq 2 in terms of a "chirality parameter" $\mathcal{Q}$. This has been formulated in a recent work as in eq 3.[12]

$$\beta = \frac{N_A k_B T \epsilon_{an}}{2\pi K_{22} v_m} \mathcal{Q} \tag{2}$$

$$\mathcal{Q} = -\sqrt{\frac{2}{3}}(Q_{xx}S_{xx} + Q_{yy}S_{yy} + Q_{zz}S_{zz})$$

$$= -\sqrt{\frac{1}{6}}[3(Q_{xx} + Q_{yy})(S_{xx} + S_{yy}) + (Q_{xx} - Q_{yy})(S_{xx} - S_{yy})] \tag{3}$$

Here, the anchoring strength ϵ_{an}, the twist elastic constant K_{22}, and molar volume v_m are more of the host characteristics, and other symbols bear usual meanings. The chirality parameter $\mathcal{Q}$ inherent to the dopant involves elements Q_{ij} of "surface chirality tensor" ***Q***, which has been defined to have no trace,[13] and elements S_{ij} of the orientational order tensor ***S***. The principal axis system (x, y, z) of the latter is usually chosen for the tensorial description of HTP, and thus the anisotropic content of HTP of a given dopant is dependent not only on how chiral the dopant is seen along each of these axes but also on how well that axis is aligned to the (local) nematic director.

(8) (a) Drake, A. F.; Gottarelli, G.; Spada, G. P. *Chem. Phys. Lett.* **1984**, *110*, 630−633. (b) Spada, G. P. Private communication.
(9) Okamoto, K.; Matsuoka, Y.; Yamagishi, A.; Hoshino, N. *Chem. Commun.* **2002**, 282−283.
(10) Hoshino, N.; Matsuoka, Y.; Okamoto, K.; Yamagishi, A. *J. Am. Chem. Soc.* **2003**, *125*, 1718−1719.
(11) (a) Ferrarini, A.; Moro, G. J.; Nordio, P. L. *Mol. Phys.* **1996**, *87*, 485−499. (b) Ferrarini, A.; Moro, G. J.; Nordio, P. L. *Phys. Rev. E* **1996**, *53*, 681−688.
(12) di Matteo, A.; Todd, S. M.; Gottarelli, G.; Solladié, G.; Williams, V. E.; Lemieux, R. P.; Ferrarini, A.; Spada, G. P. *J. Am. Chem. Soc.* **2001**, *123*, 7842−7851.
(13) A tensorial approach that covers also chiral, isotropic state is given in ref 1. See also (a) Kuball, H.-G.; Brüning, H.; Müller, T.; Türk, O.; Schönhofer, A. *J. Mater. Chem.* **1995**, *5*, 2167−2174. (b) Osipov, M. A.; Kuball, H.-G. *Eur. Phys. J. E* **2001**, *5*, 589−598.

Chart 2. (a) A Model *P*-1,1′-Binaphthyl Dopant and Its Axis Labeling for Equations 4−6, (b) a Schematic Model for a Metal Complex Dopant of Δ-[Ru(acac)$_2$L] Type and the Most Probable Principal Axis System for the Ordering Tensor, and (c) a Space-Filling Model of Δ-Ru-2 Viewed down along Its *x* Axis or C_2 Symmetry Axis

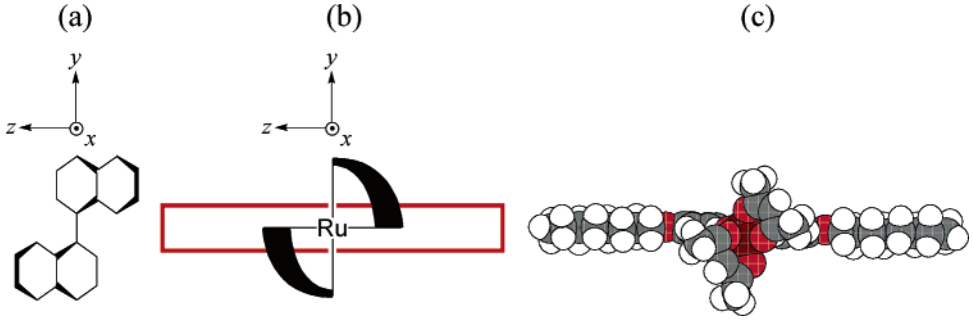

It is possible to compute all four independent elements in eq 3 and evaluate $\mathcal{Q}$ (and then β), and such an approach has been reported on bridged 1,1′-biaryls,[1,2] alkyl aryl sulfoxide,[5a] and helicenes.[5b] On the other hand, a rational design to drop a term or two in eq 3 serves to make the theory more transparent. It is recalled for this purpose that a set of equations have been derived to evaluate Q_{ii} elements on the basis of the shape model for 1,1′-biaryls,[11a] in which the system is approximated as a pair of rectangular panels of side l and area σ, connected by a segment of length $2l_0$ and rotated by an angle δ. The axis labels are shown for a model *P*-1,1′-biphenyl in Chart 2a.

$$Q_{xx} = -\sqrt{6}\sigma(l_0 + l/2)\sin(\delta/2)\cos(\delta/2) \quad (4)$$

$$Q_{yy} = 0 \quad (5)$$

$$Q_{zz} = \sqrt{6}\sigma(l_0 + l/2)\sin(\delta/2)\cos(\delta/2) \quad (6)$$

It is useful to note that the surface elements about the connecting (stereogenic) axis y, Q_{xx} and Q_{zz}, are maximized in magnitude at $\delta = 90°$. However, the chirality parameter $\mathcal{Q}$ is brought to nearly zero due to unfavorable orientational distribution at this conformation in the case of this prototype dopant. We reasoned that, if the dopant is elongated along its z axis, S_{zz} [$=-(S_{xx} + S_{yy})$] should be maximized and only the first term in eq 3 survives when biaxial ordering is suppressed ($S_{xx} \approx S_{yy}$). Since the component Q_{yy} (=0) does not harm Q_{xx}, this should be effective in holding HTP large in size.

The strategy "to elongate along z, while $\delta = 90°$ is maintained" can be achieved most easily in a metal complex of Δ-[M(acac)$_2$L] type in Chart 2b, where the Δ-(acac)$_2$ blades (in black) can be viewed as a compressed biaryl ($l_0 = 0$) open rigidly at a right angle with the rodlike ligand L attached as a backbone (in red). It can be predicted that $Q_{xx} < 0$, $Q_{yy} \approx 0$, and $Q_{zz} \approx -Q_{xx}$ for this Δ-isomer, approximating L as flat within the xz plane. This way, the "lateral" chirality could be effectively transmitted to the longitudinal component (with sign inverted) in a uniaxially orienting potential. This scheme for high HTP with predicted sign is in accord with the fact that the helical axis is to develop in a direction perpendicular to the director in the case of chiral nematics. Equation 3 can now be simplified to

$$\mathcal{Q} \approx \sqrt{\frac{2}{3}}Q_{xx}(S_{zz} - S_{xx}) \quad (7)$$

If further approximation is made for full uniaxiality, only the first term is left: $\mathcal{Q} \approx (3/2)^{1/2}Q_{xx}S_{zz}$.

Synthesis and Optical Resolution of the Ru(III) Complexes. Synthetic procedures for the alkoxylation of dibenzoylmethane and the preparation of mixed chelate complexes of Ru(III) are known in the literature. Coordination of mixed 1,3-diketonate ligands was achieved in this study by the use of bisacetylacetonate starting material [Ru(acac)$_2$(CH$_3$CN)$_2$]$^+$, acetonitrile sites of which were replaced under a reducing condition by a weaker dibenzoylmethanate ligand, and subsequent reoxidation. It proved that the neutral products can be fully resolved into the enantiomers by using an HPLC column packed with a clay mineral modified with Δ-[Ru(phen)$_3$]$^{2+}$. Once the material had been purified chemically by a usual silica-based column (while racemic), the optical resolution was accomplished with further separation of impurities. Two major peaks off this chiral column were well-separated from each other to the "baseline" level in the very first run of elution with chloroform−methanol.

Although the mechanism of enantioselectivity of this chromatography is not well understood, it has been shown previously that Δ-enantiomers of certain Ru(III) tris-chelates and mixed 1,3-diketonates were more strongly adsorbed, while the situation was reverse for tris-chelates of Cr(III) and Co(III).[14] The CD spectrum is diagnostic of the stereoisomerism in the case of [Ru(acac)$_3$]. Three absorption bands in the 250−550-nm range were ascribed theoretically to the excited states admixed of the ligand $\pi-\pi^*$ triplets and singlets and ligand-to-metal charge transfer (LMCT) states for this open-shell complex (d^5, $S = 1/2$).[15] It was also deduced that the LMCT causes splitting of the ground-state sublevels. An intense positive band at 275 nm, followed by a negative and a positive band, in its CD spectrum was then ascribed to the ligand $\pi-\pi^*$ exciton band of the Δ-form, which was corroborated later by the single crystal determination of this absolute configuration.[16] Our complexes are

(14) Kashiwara, S.; Takahashi, M.; Nakata, M.; Taniguchi, M.; Yamagishi, A. *J. Mater. Chem.* **1998**, *8*, 2253−2257.
(15) Kobayashi, H.; Matsuzawa, H.; Kaizu, Y.; Ichida, A. *Inorg. Chem.* **1987**, *26*, 4318−4323.

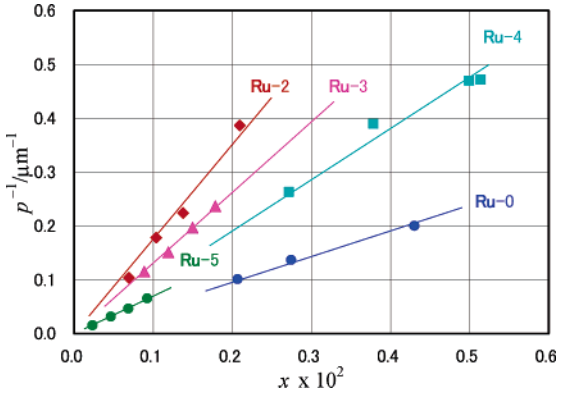

Figure 1. Plots of the inverse helical pitch (p^{-1}) vs mole fraction of the dopant (x) for MBBA* materials obtained by doping with either Δ-**Ru-*n*** (n = 0 and 4) or Λ-**Ru-*n*** (n = 2, 3, and 5).

of lower symmetry, where the degeneracy of d_π orbitals must be partially removed. But the basic feature of the electronic states or admixture of low-lying LMCT state(s) would be retained, as an acac ligand has been replaced by L-*n* having a more extended π system, and in turn the characteristic CD spectral pattern of the acac complex would be applicable. Thus, by analogy to [Ru(acac)$_3$], the first major fraction of **Ru-*n*** off the chiral column exhibiting a negative CD band over the 250−310-nm range, followed by a positive and a negative band, was assigned in the present study to the Λ-enantiomer of each complex and the second major fraction showing a mirroring CD pattern to its antipode.

This elution pattern seems to be common to a group of complexes of trivalent metal ions containing the M(acac)$_2$ unit, and a Cr(III) analogue of **Ru-3** was resolved in a similar manner.[17] The first and second fractions were taken to be its Λ- and Δ-enantiomers on the basis of their diagnostic CD spectra around 300 nm (negative and positive, respectively), the assignment of which has been established in the literature.[18]

Determination of HTP. The optical resolution of Ru(III) complexes was carried out in such small quantities that their bulk properties, including possible mesomorphism, have not been fully characterized. However, they proved to be soluble in MBBA, and the MBBA* materials displayed fingerprint textures, indicative of the induction of chiral nematic phases, even at such a low doping level as 0.1 wt %.

Figure 1 compiles pitch data for the helical superstructure obtained by the Cano method, plotting the inverse of measured pitch length (p^{-1}) against the mole fraction (x) of the dopant. The magnitude of HTP ($|\beta_M|$) is given by the initial slope of such a plot according to eq 1. The sign of β_M was determined by the CD spectrum of MBBA* material (vide infra) for each dopant, by testing both of the enantiomers in some cases, and the results collected at 25.0 °C are listed in Table 1. We note that these somewhat tedious procedures are necessary for eliminating the concentration effect. Determinations at one finite concentration were

Table 1. Values for HTP (β_M)[a] of Ru-*n* in MBBA at 25.0 °C, CD Spectral Data (Δε),[b] and the Dissymmetry Ratio (Δε/ε) Relevant to Their Optical Resolution

	β_M/μm^{-1}		Δε/mol^{-1} dm^3 cm^{-1}		(Δε/ε)	
n	Λ	Δ	Λ	Δ	× 10^4	λ/nm
0	*c*	−48	11.0	−11.7	8.22	333
2	176	*c*	20.8	−17.7	7.79	337
3	131	−133	16.1	−16.6	6.67	339
4	(84)	−95	10.6	−10.7	6.78	343
5	70	(−38)	10.7	−11.7	7.57	345

[a] The + and − values indicate that *P*- and *M*-helical superstructures are induced, respectively. The values in parentheses are estimates based on one sample. In no case was the concentration greater than 0.6 mol %. [b] Measured in methanol at room temperature. [c] Not determined.

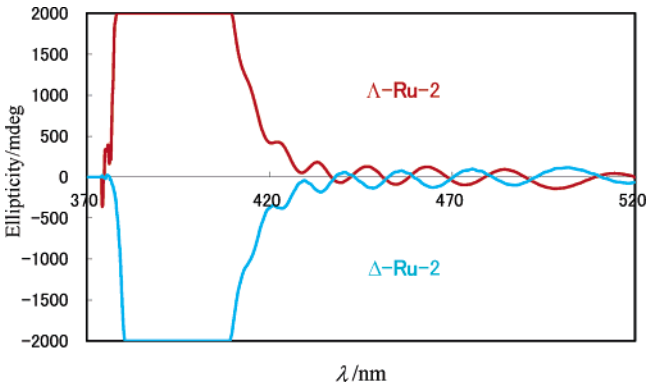

Figure 2. The ICD spectra for MBBA* materials obtained by doping with Δ- (blue) or Λ-**Ru-2** (red) at 0.30 wt % levels (recorded with normal incidence, i.e. along the helical axis, in a 25 μm cell).

inclined to involve errors and to report lower HTP in the present study.

Immediate attention is drawn to the case of Λ-**Ru-2**, for which the value of β_M is the largest (1.8 × 10^2 μm^{-1}). This is one of most powerful dopants reported, and we should be able to observe selective reflection in the visible spectral range at the doping level of 1−2 mol %. Others also rank relatively high in comparison to conventional organic dopants. Two further points are noted: (a) Δ- and Λ-enantiomers of **Ru-*n*** induce *M*- and *P*-helical superstructures, respectively, regardless of the mode of chain appendage (*n*), and (b) the magnitude of HTP appears to be correlated with *n* in a manner of gradual decrease after the initial jump upon substitution.

CD Spectroscopy. It should be noted that the signs of β_M values in Table 1 have been confirmed by measuring the ICD spectrum for each specimen in the chiral nematic phase and are consistent with our previous work.[10] Figure 2 shows an example of intense signals mirroring each other in the wavelength range for the imine chromophore of MBBA. The helical pitch is longer than this for all of the MBBA* materials, and the negative ICD indicates that the left-handed helical structure has been induced (and vice versa) in the host director field.[19]

A description of the light propagation through chiral nematic liquid crystals has been thoroughly worked out. The ICD intensity data were used in this study to check the

(16) Matsuzawa, H.; Ohashi, Y.; Kaizu, Y.; Kobayashi, H. *Inorg. Chem.* **1988**, *27*, 2981−2985.
(17) Yamagishi, A.; Matsuoka, Y. Unpublished results.
(18) (a) Minor, S.; Witte, G.; Everett, G. W. *Inorg. Chem.* **1976**, *15*, 2052−2055. (b) Mason, S. F.; Peacock, R. D.; Prosperi, T. *J. Chem. Soc., Dalton Trans.* **1977**, 702−704.
(19) (a) Pirkle, W. H.; Rinaldi, P. L. *J. Org. Chem.* **1980**, *45*, 1379−1382. (b) Rinaldi, P. L.; Naidu, M. S. R.; Conaway, W. E. *J. Org. Chem.* **1982**, *47*, 3987−3991. (c) Rinaldi, P. L.; Wilk, M. *J. Org. Chem.* **1983**, *48*, 2141−2146.

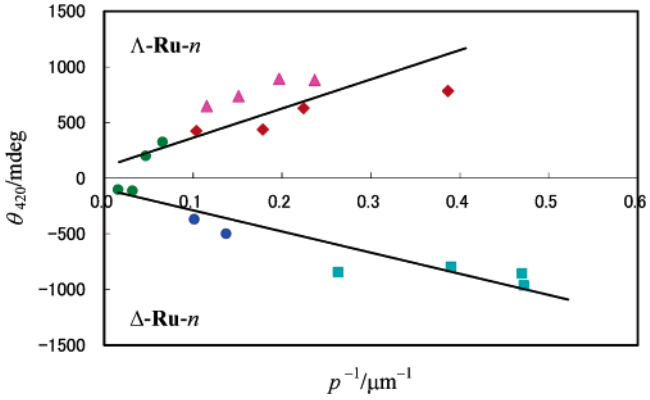

Figure 3. Plots of the ICD intensity (at 420 nm) vs p^{-1} for MBBA* materials obtained by doping with either Δ-**Ru-*n*** (n = 0, 4, and 5) or Λ-**Ru-*n*** (n = 2, 3, and 5). Symbols are the same as in Figure 1.

consistency of our interpretation. The chiral nematics having long pitches act as helically stacked slices of linearly birefringent and dichroic medium to the UV−vis light passing along the helical axis, and in this situation the observed ellipticity is proportional to the inverse pitch (p^{-1}) (when other parameters are set constant) according to Sackmann and Voss.[20] Selected examples of such data are plotted in Figure 3. The linear relationship in the ICD intensity to p^{-1} can be recognized, regardless of the dopant used, although the ICD data extracted from the band edges are pretty scattered. Thus, the behavior of the MBBA* materials of very low doping levels employed in this study is fully consistent with the prediction.

Structure−Performance Relations. Theoretical interpretations for the structure−HTP correlation will require knowledge of the chirality *and* orientational characteristics of the systems. We have postulated the "chiral blade model" in our previous publication to account for the high power of metal-centered chirality in [Ru(acac)$_2$(obpy)].[10] For this precursor complex with the rodlike ligand obpy that is mesomorphic by itself,[9] it was inferred that it assists the orientational matching of the dopant to host molecules, thereby ensuring the twisting power of the two acac blades. This concept has been lined with theoretical terms with the aid of the shape model by Ferrarini et al. as described above. The twist sense correlation, Δ−*M* and Λ−*P*, found and confirmed in this study, is in exact accord with eq 7, which predicts $\mathcal{Q} < 0$ (hence $\beta < 0$) for Δ-enantiomers (and vice versa).

It is enlightening that the magnitudes of HTP are very close to each other between the two-chain dopants, Δ-**Ru-2** and Δ-[Ru(acac)$_2$(obpy)] (-1.7×10^2 μm^{-1}),[10] both of which would order uniaxially and carry basically the same chirality element. The three-blade parent, Δ-[Ru(acac)$_3$], where nominally three pairs of the blades can operate, has been reported to possess a lower power (-102 μm^{-1}).[8] Perhaps its small size and a more isometric shape would cause too fast tumbling for their effect to be fully exploited. The usefulness of the terminal alkyl chains is also illuminated by the result that their elimination leads to the diminished power in Δ-**Ru-0** (-48 μm^{-1}). Addition of extra chains in Δ-**Ru-3**, **-4**, and **-5** gradually lowered their twisting power. Assuming that these chains populate the *xz* plane on average and make L-*n* virtually flattened (in liquid crystals), the effect can be interpreted as rendering the lateral elements of the ordering matrix, S_{xx} and S_{yy}, more and more significant with increasing n. This happens at the expense of S_{zz}, and the $\mathcal{Q}$ value will become less and less negative through eq 7. Incorporating some degree of biaxial order ($|S_{xx}| < |S_{yy}|$) would promote the effect. The last alkyl chain is most likely to go in the peripheral position for **Ru-5**, and this dopant may be regarded more as disklike. Table 2 illustrates how the dopant performance of a series of Δ-**Ru-*n*** complexes is navigated by eq 7, by employing plausible values of order parameters deduced from the molecular structure.

Molecular Calculations—An Approach to the Chirality Recognition. The above prediction that $Q_{xx} < 0$ for Δ-**Ru-*n*** is inherited from eq 4 for a model *P*-1,1′-biaryl species and expresses the shape factor of Δ-(acac)$_2$ moiety. So far the argument has been grounded on the excluded volume effect in the nematics. Attractive term(s) involved in the guest−host interactions of chemical interest are implicitly treated by the parameter ϵ_{an} in eq 2, which in fact governs the magnitude of HTP. In an effort to obtain a microscopic view and to clarify the mechanism of chirality recognition in the locus of metal centers, we also conducted molecular calculations using a *Gaussian98* package[21] for a model Al(III) analogue of Δ-**Ru-2**.

About 60 cases of initial configurations were tested, e.g. one MBBA molecule was either laid behind or stood across the ligand L-2, either parallel or antiparallel to the other placed across the complex, with the two octyl chains on the complex either extended lengthwise or set away from the (acac)$_2$ unit, and so on. The stable structure of Δ-**Al-2** alone was calculated for comparison and turned out to involve the terminal chains sticking out and away from the blades, which is natural for the isolated state. However, the configuration for the cluster of Δ-**Al-2** with two MBBA molecules converged with the extended conformation for the tails and with the MBBA molecules forming a mutually negative twist over Δ-**Al-2** ($\theta = -22°$).[22] Figure 4 shows the energy-minimized structure for [Δ-**Al-2** + 2MBBA]. It appears here that the 4-butylaniline moiety of one MBBA (X) is nearly riding over the back portion of L-2, and the core part of the other (Y) is situated in a space sectored by the lower acac

(20) Sackmann, E.; Voss, J. *Chem. Phys. Lett.* **1972**, *14*, 528−532.

(21) Frisch, M. J.; Trucks, G. W.; Schlegel, H. B.; Scuseria, G. E.; Robb, M. A.; Cheeseman, J. R.; Zakrzewski, V. G.; Montgomery, J. A.; Stratmann, R. E.; Burant, J. C.; Dapprich, S.; Millam, J. M.; Daniels, A. D.; Kudin, K. N.; Strain, M. C.; Farkas, O.; Tomasi, J.; Barone, V.; Cossi, M.; Cammi, R.; Mennucci, B.; Pomelli, C.; Adamo, C.; Clifford, S.; Ochterski, J.; Petersson, G. A.; Ayala, P. Y.; Cui, Q.; Morokuma, K.; Salvador, P.; Dannenberg, J. J.; Malick, D. K.; Rabuck, A. D.; Raghavachari, K.; Foresman, J. B.; Cioslowski, J.; Ortiz, J. V.; Baboul, A. G.; Stefanov, B. B.; Liu, G.; Liashenko, A.; Piskorz, P.; Komaromi, I.; Gomperts, R.; Martin, R. L.; Fox, D. J.; Keith, T.; Al-Laham, M. A.; Peng, C. Y.; Nanayakkara, A.; Challacombe, M.; Gill, P. M. W.; Johnson, B. G.; Chen, W.; Wong, M. W.; Andres, J. L.; Gonzalez, C.; Head-Gordon, M.; Replogle, E. S.; Pople, J. A. *Gaussian98*, Revision A.11; Gaussian, Inc.: Pittsburgh, PA, 2001.

(22) Defined as θ_p = O(methoxy)^X − N(imine)^X − N^Y − O^Y and θ_a = O^X − N^X − O^Y − N^Y for initially parallel and antiparallel states, respectively. The structure shown in Figure 4 ($\theta_a = -22°$) was derived by the DFT calculations from an initial arrangement where X is parallel to L-2 and Y is antiparallel to X, in an attempt to imitate the nematic state. Some HF calculations also yielded $\theta_p = -34°$.

Table 2. Comparison between the β_M Values Determined Experimentally for Δ-Ru-*n* and Estimated Values of β[a] Assuming Plausible Orientational Order

n	$\beta_M/\mu m^{-1}$	$\beta/\mu m^{-1}$	$\mathcal{Q}/Å^3$	S_{xx}	S_{yy}	S_{zz}	behavior
2	−180	−156	−75	−0.4	−0.4	0.8	uniaxial rod
3	−130	−130	−63	−0.3	−0.4	0.7	biaxial rod
4	−95	−98	−47	−0.15	−0.45	0.6	biaxial rod, less ordered
5	−70	−72	−35	−0.05	−0.45	0.5	biaxial rod/disk
0	−48	−52	−25	0	−0.4	0.4	*b*

[a] To input in eq 7, a test parameter $Q_{xx} = -77$ Å^3 has been employed for the Δ-(acac)$_2$ moiety, which was calculated from eq 4 with $\sigma = 25$ Å^2, $l = 5$ Å, $l_0 = 0$, and $\delta = 90°$. The proportionality constant between β and $\mathcal{Q}$ in eq 2 was estimated from literature values appropriate for MBBA at 300 K (ref 11) and set constant or unadjusted for different orientational behaviors. [b] The principal axis system may actually switch for unsubstituted Δ-**Ru-0**, but the behavior as a less ordered biaxial rod/disk would also reproduce the experimental result under the current assumptions.

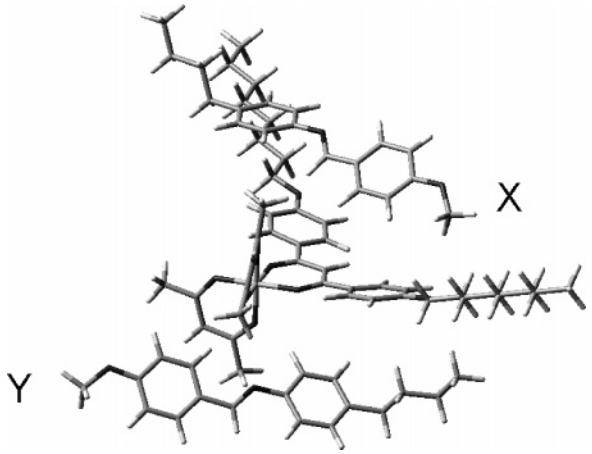

Figure 4. An angled view of the energy-minimized structure of [Δ-**Al-2** + 2MBBA], showing the mutually left-handed orientation of two MBBA molecules.

ligand below L-2. It is notable that the left-handed twist sense has come out to be the same as that of HTP found experimentally for the Δ-**Ru-*n***, while the present molecular calculations are by no means to simulate the liquid crystalline state.[22]

Concluding Remarks. Chiral mixed 1,3-diketonate complexes of Ru(III) have thus proved to be a remarkably powerful twister for MBBA, and key features for interpreting the structure−performance correlations have been extracted. It should be pointed out that there exists the literature case of TADDOLs (α,α,α′,α′-tetraaryl-1,3-dioxolan-4,5-dimethanols)[23] that truly stands out; their values for HTP range from ca. 100 μm^{-1} for the original TADDOL to the highest of 405 μm^{-1} (in 5CB, 24−34°C) for one of the derivatives with four large 9-phenanthryl groups as α-substituents. An apparently common feature in crystal structures of TADDOLs is the stereochemical arrangement of a pair of axial aryl groups relative to the equatorial pair, although its significance in relation to the high HTPs is not clear. Generally speaking, (*R*,*R*)-TADDOLs somehow induce the same sense of helicity as *P*-1,1′-binaphthols, and their anions as ligands exhibit also the same stereoselectivity in organometallic reactions. It is rather likely that the involvement of hydrogen bonding interaction to host bi(cyclohexyl)carbonitrile molecules is important, since these compounds are diols, and in fact, reduction or removal of the H-bond-donating ability leads to diminished HTP. A large derivative in which two *M*-1,1′-binaphthyl derivatives are doubly connected by *p*-xylylene groups at their 2- and 2′-positions and elongated in a direction corresponding to the *x* axis in Chart 2a has been reported; it shows a very high HTP (−240 μm^{-1}), but its performance is not a simple sum of the chiral components.[24] On the other hand, our dopants are monomeric and coordinatively saturated. Therefore, they should be able to serve as a relatively innocent source of chirality, and the packing entropy alone would drive the materials to wind up once the orientational and diffusion characteristics are set right. In fact, this is the charm of the phenomenon: the chiral center of such a low density as one in several hundreds of molecules can still be recognized and be reported upon by the *fluid* liquid crystal system.

The solubility properties of metal complex dopants remain a point of consideration. A chirooptical application of a wide range of Cr(III) 1,3-diketonates has been reported recently, in which solubility problems and improvements are alluded to.[25] The Cr(III) analogues of **Ru-*n*** are under pursuit in our laboratories, since the dissymmetry ratios of the latter may also be raised (they are currently on the order of 10^{-4}; Table 1). Complexes of suitable metals will also allow for the application of NMR or EPR[26] spectroscopy in the experimental determination of order parameters, which is highly desirable. In addition, there seems to be a revived interest in enantioselective oxidation catalysis utilizing the stereogenic nature of transition metals such as Ru(II).[27] Chiral liquid crystals, locally fluid and still structured on the macroscopic (and adjustable) scale, could be worth exploring as partially ordered reaction media. Here chiral tris-chelate complexes could potentially bear dual tasks of a chiral dopant and a catalyst.

Experimental Section

Synthesis. Synthetic procedures for alkylated dibenzoylmethanes, HL-*n*, involving a coupling reaction between derivatives of acetophenone and methyl benzoate, and the Ru(III) mixed chelate complexes have been described in the literature,[28,29] from which the present preparations were adapted. A representative case of $n = 3$ is described below, and lists of analytical data for others will follow. Dibenzoylmethane (HL-0) from Kanto Kagaku Co., Ltd. was used as received.

(23) Kuball, H.-G.; Weiss, B.; Beck, A. B.; Seebach, D. *Helv. Chim. Acta* **1997**, *80*, 2507−2514.

(24) Proni, G.; Spada, G. P.; Lustenberger, P.; Welti, R.; Diederich, F. *J. Org. Chem.* **2000**, *65*, 5522−5527.

(25) (a) Anzai, N.; Machida, S.; Horie, K. *Liq. Cryst.* **2003**, *30*, 359−366. (b) Anzai, N.; Horie, K. *EKISHO, J. Jpn. Liq. Cryst. Soc.* **2004**, *8*, 26−35.

(26) Hoshino, N.; Kodama, A.; Shibuya, T.; Matsunaga, Y.; Miyajima, S. *Inorg. Chem.* **1991**, *30*, 3091−3096.

(27) Chavarot, M.; Ménage, S.; Hamelin, O.; Charnay, F.; Pécaut, J.; Fontecave, M. *Inorg. Chem.* **2003**, *42*, 4810−4816.

3,4-Dioctyloxyacetophenone. This material was prepared by refluxing 200 mL of 2-butanone solution of 5.0 g (32 mmol) of 3,4-dihydroxyacetophenone, 7.4 g (66 mmol) of KOBu^t, and 11 mL (66 mmol) of 1-bromooctane. A pale yellow powdery product was obtained after usual workup of the resulting orange solution by extracting with 150 mL of dichloromethane, drying with magnesium sulfate, rotary evaporation, and finally recrystallizing from 300 mL of 5:1 hexane−ethanol. Yield: 72%. Mp: 57.5−58.3 °C.^{1}H NMR (400 MHz, $CDCl_3$): δ (ppm) 7.53 (d, J = 8.4 Hz, 1H), 7.51 (s, 1H), 6.86 (d, J = 8.4 Hz, 1H), 4.02 (t, J = 6.2 Hz, 4H), 2.56 (s, 3H), 1.80 (m, 4H), 1.23−1.34 (m, 20H), 0.87 (t, J = 7.2 Hz, 6H).

1-(3,4-Dioctyloxyphenyl)-3-(4′-octyloxyphenyl)propane-1,3-dione (HL-3).[28f] A 5.0 g quantity of 3,4-dioctyloxyacetophenone (13 mmol) prepared above was reacted with an excess of NaH (1.27 g, 53 mmol) in 150 mL of DME under nitrogen atmosphere. An equimolar amount of methyl 4-octyloxybenzoate[28b] was added, and the mixture was refluxed overnight. After the reaction was quenched carefully with ice−water, the same workup and recrystallization as above led to isolation of again a pale yellow powdery product. Yield: 71%. Mp: 73.0−73.3 °C. ^{1}H NMR (400 MHz, $CDCl_3$): δ (ppm) 17.14 (s, 1H), 7.94 (d, J = 8.4 Hz, 2H), 7.55 (m, 2H), 6.95 (m, 3H), 6.72 (s, 1H), 4.02 (t, J = 6.6 Hz, 6H), 1.85 (m, 6H), 1.30 (m, 30H), 0.88 (t, J = 6.8 Hz, 9H).

HL-2. Yield: 54%, of a pale yellow powder. Mp: 83.5−84.5 °C. ^{1}H NMR (400 MHz, $CDCl_3$): δ (ppm) 17.15 (s, 1H), 7.94 (d, J = 8.9 Hz, 4H), 6.95 (d, J = 8.9 Hz, 4H), 6.72 (s, 1H), 4.02 (t, J = 6.6 Hz, 4H), 1.80 (m, 4H), 1.45 (m, 4H), 1.27 (m, 16H), 0.88 (t, J = 6.8 Hz, 6H).

HL-4. Yield: 26%, of a yellow powder. Mp: 78.2−79.4 °C. ^{1}H NMR (400 MHz, $CDCl_3$): δ (ppm) 17.08 (s, 1H), 7.55 (m, 4H), 6.90 (d, J = 8.9 Hz, 2H), 6.70 (s, 1H), 4.08 (t, J = 6.8 Hz, 8H), 1.85 (m, 8H), 1.33−1.47 (m, 40H), 0.89 (t, J = 6.9 Hz, 12H).

HL-5. Yield: 16%, of a yellow viscous oil. ^{1}H NMR (400 MHz, $CDCl_3$): δ (ppm) 17.13 (s, 1H) 7.56 (m, 2H), 7.16 (s, 2H), 6.90 (d, J = 8.9 Hz, 1H), 6.67 (s, 1H), 4.05 (t, J = 6.9 Hz, 10H), 1.80 (m, 10H), 1.28−1.48 (m, 50H), 0.86 (t, J = 6.9 Hz, 15H).

[1-(3,4-Dioctyloxyphenyl)-3-(4′-octyloxyphenyl)propane-1,3-dionato][bis(pentane-2,4-dionato)]ruthenium(III) (Ru-3).[29] A 0.26 g (0.40 mmol) amount of the starting Ru(III) complex [Ru(acac)$_2$(CH$_3$CN)$_2$]ClO$_4$,[29] 0.25 g (0.40 mmol) of the ligand HL-3, 0.053 g of Zn powder, and 0.059 g of $KHCO_3$ were dissolved in a mixture of 40 mL of ethanol and 2 mL of water, and the mixture heated at reflux overnight. The solution was cooled, filtered through Celite, and evaporated. The residue was dissolved in 50 mL of chloroform and refluxed overnight again with 5−10 mL of an aqueous solution containing 0.1−0.2 g of $AgNO_3$. The solution was evaporated to dryness, and the products were purified by HPLC (Shiseido Capcell Pak C18) eluting with methanol, which yielded the desired product upon evaporation. **Caution:** *the perchlorate salt should be handled with care.* Yield: 24%, of a dark red pasty solid. Mp: ca. 62 °C. FAB-MS: calcd for $C_{49}H_{73}O_9Ru$ $[M]^+$, $[M - acac]^+$ m/z = 907.4, 808.3, found 907, 808. ^{1}H NMR (400 MHz, $CDCl_3$): δ (ppm) 13.02 (s, 1H), 12.80 (m, 2H), 11.58 (s, 1H), 6.18 (m, 2H), 5.92 (d, J = 8.0 Hz, 1H), 4.06 (t, J = 6.8 Hz, 6H), 1.98−2.24 (m, 6H), 1.28−1.64 (m, 30H), 0.93 (t, J = 6.2 Hz, 9H), −1.49 (s, 3H), −3.14 (s, 3H), −3.83 (s, 3H), −5.53 (s, 3H), −25.48 (s, 1H), −28.58 (s, 1H), −40.42 (s, 1H).

Ru-0: Yield: 38%, of a deep red powder. Mp: 240 °C (dec). FAB-MS: calcd for $[M]^+$, $[M - acac]^+$ m/z = 522.5, 423.4, found 523, 424. ^{1}H NMR (400 MHz, $CDCl_3$): δ (ppm) 12.82 (d, J = 6.7 Hz, 4H), 9.96 (t, J = 7.0 Hz, 2H), 6.58 (m, 4H), −2.46 (s, 6H), −4.87 (s, 6H), −27.58 (s, 2H), −40.97 (s, 1H). Anal. Calcd for $C_{25}H_{25}O_6Ru \cdot 1.5H_2O$: C, 54.64; H, 5.12. Found: C, 54.14; H, 4.94.

Ru-2: Yield: 32%, of a dark red powder. Mp: ca. 85 °C. FAB-MS: calcd for $[M]^+$, $[M - acac]^+$ m/z = 779.0, 679.8, found 779, 680. ^{1}H NMR (400 MHz, $CDCl_3$): δ (ppm) 12.69 (s, 4H), 6.22 (m, 4H), 4.05 (t, J = 6.5 Hz, 4H), 1.94−2.14 (m, 4H), 1.36−1.56 (m, 20H), 0.93 (t, J = 6.8 Hz, 6H), −2.69 (s, 6H), −4.87 (s, 6H), −27.49 (s, 2H), −38.30 (s, 1H). Anal. Calcd for $C_{41}H_{57}O_8Ru \cdot H_2O$: C, 61.79; H, 7.46. Found; C, 61.42; H, 7.60.

Ru-4: Yield: 18%, of a dark red pasty solid. Mp: ca. 85 °C. FAB-MS: calcd for $C_{57}H_{89}O_{10}Ru$ $[M]^+$, $[M - acac]^+$ m/z = 1035.4, 936.3, found 1035, 936. ^{1}H NMR (400 MHz, $CDCl_3$): δ (ppm) 13.20 (s, 2H), 11.62 (s, 2H), 6.00 (m, 2H), 4.03 (t, J = 7.1 Hz, 8H), 1.16−2.08 (m, 48H), 0.91 (m, 12H), −1.83 (s, 6H), −4.42 (s, 6H), −26.59 (s, 2H), −42.36 (s, 1H).

Ru-5: Yield: 15%, of a dark red pasty solid. Mp: ca. 76 °C. FAB-MS: calcd for $C_{65}H_{105}O_{11}Ru$ $[M]^+$, $[M - acac]^+$ m/z = 1163.6, 1064.5, found 1163, 1064. ^{1}H NMR (400 MHz, $CDCl_3$): δ (ppm) 13.32 (s, 1H), 11.81 (s, 2H), 11.31 (s, 1H), 5.77 (m, 1H), 3.99−4.25 (m, 10H), 1.86−2.65 (m, 10H), 1.26−1.56 (m, 50H), 0.90 (m, 15H), −1.58 (s, 3H), −2.43 (s, 3H), −4.16 (s, 3H), −4.83 (s, 3H), −25.92 (s, 1H), −27.76 (s, 1H), −43.20 (s, 1H).

Physical Measurements and Optical Resolution. For characterization purposes, the ^{1}H NMR spectra were recorded for the paramagnetic Ru(III) complexes (while racemic), with a normal 5 ppm offset but with a large sweep width (either 40 or 50 kHz, JEOL-AL400), by referencing the literature, and all of the protons were detected.[30] Elemental analyses were not reliable due to the hygroscopic nature of the complexes. In addition, they were isolated often as partially amorphous solids,[31] except for **Ru-0**. We resorted to FAB mass spectroscopy (JEOL JMS-HX110 and JMS-700TZ) for their identification, and the parent molecular ion and its fragment were detected commonly to all of the complexes prepared.

The desired fraction from above was further run on a column of Ceramospher Chiral RU-1 for optical resolution eluting with chloroform−methanol at a flow rate of 0.4 mL min^{-1}. Two major peaks were clearly separated with an intervening span of baseline on the chromatogram. Only these abundant fractions were collected and identified as Λ- and Δ-enantiomers from their CD spectra (vide supra). Slower minor fraction(s) were then discarded. It was confirmed that both of the two fractions from the chiral column

(28) 4-Octyloxyacetophenone: (a) Tantrawong, S.; Styring, P.; Goodby, J. W. *J. Mater. Chem.* **1993**, *3*, 1209−1216. Methyl 4-octyloxybenzoate: (b) Lai, C. K.; Tsai, C.-H.; Pang, Y.-S. *J. Mater. Chem.* **1998**, *8*, 1355−1360. Methyl 3,4-dioctyloxybenzoate: (c) Percec, V.; Holerca, M. N.; Magonov, S. N.; Yardley, D. J. P.; Ungar, G.; Duan, H.; Hudson, S. D. *Biomacromolecules* **2001**, *2*, 706−728. Methyl 3,4,5-trioctyloxybenzoate: (d) Serrette, A. G.; Lai, C. K.; Swager, T. M. *Chem. Mater.* **1994**, *6*, 2252−2268. HL-2: (e) Tantrawong, S.; Styring, P.; Goodby, J. W. *J. Mater. Chem.* **1993**, *3*, 1209−1216. (f) Ohta, K., Muroki, H.; Hatada, K.; Takagi, A.; Ema, H.; Yamamoto, I.; Matsuzaki, K. *Mol. Cryst. Liq. Cryst.* **1986**, *140*, 163−177. HL-3: (g) Poelsma, S. N.; Servante, A. H.; Fanizzi, F. P.; Maitlis, P. M. *Liq. Cryst.* **1994**, *16*, 675−685. HL-4: (h) Ohta, K.; Ema, H.; Muroki, H.; Yamamoto, I.; Matsuzaki, K. *Mol. Cryst. Liq. Cryst.* **1987**, *147*, 61−78. It is noted that ref 28g also discusses the reported mesomorphism of HL-2 (28f) and HL-4 (28h). HL-5: (i) Zheng, H.; Lai, C. K.; Swager, T. M. *Chem. Mater.* **1995**, *7*, 2067−2077.

(29) Kasahara, Y.; Hoshino, Y.; Shimizu, K.; Sato, G. P. *Chem. Lett.* **1990**, 381−384.

(30) (a) Yamagishi, A.; Sasa, N.; Taniguchi, M.; Endo, A.; Sakamoto, M.; Shimizu K. *Langmuir* **1997**, *13*, 1689−1694. (b) Baird, I. R.; Rettig, S. J.; James, B. R.; Skov, K. A. *Can. J. Chem.* **1999**, *77*, 1821−1833. (c) Koiwa, K.; Masuda, Y.; Shono, J.; Kawamoto, Y.; Hoshino, Y.; Hashimoto, T.; Natarajan, K., Shimizu, K. *Inorg. Chem.* **2004**, *43*, 6215−6223.

(31) The melting temperatures reported for **Ru-3**, **-4**, and **-5** are rough measures taken by microscopic observation of cast films, thoroughly dried.

showed identical mass spectra. The CD spectra were recorded on a JASCO J-720 spectropolarimeter.

The helical pitch lengths in the induced chiral nematic phases were measured by the Cano method.[32] An amount of solid sample of the dopant was weighed accurately on the scale of 10 mg (once or twice for each dopant) and dissolved in 10 mL of methanol, for which the extinction coefficient ϵ was determined for UV−vis absorption maximum. Aliquots of 1−4 mL of this stock solution were taken out and thoroughly evaporated before MBBA was weighed in for the pitch measurement. The Cano experiments were repeated with two or three wedge cells of different tangencies (EHC) and the objective micrometer readings were taken for several spots of Grandjean−Cano steps and averaged. Uncertainty in the concentration parameter may be greater, while the variances in p^{-1} were comparable to the cell specifications (±5%). The plots in Figure 1 yield the lowest estimates for $|\beta_M|$ in that all of the dopants are treated as enantiomerically pure. For the ICD spectral measurements, glass cells of 25 μm gap (parallel buffed) were used, and the normal incidence was checked by rotating the cell for each sample.

Computations. Geometry optimization was performed using the *Gaussian98* program.[21] The Ru(III) center was replaced by Al(III) to avoid any complexity arising from d-electrons. In the first step, the minimal STO-3G basis set was used at the HF level, and the structure was optimized using HF/3-21G**. It is emphasized that the optimization was carried out at each step with no restrictions, except for fixing six Al−O distances. At first, the optimized structure of a cluster of Δ-**Al-2** and MBBA molecules was calculated successively; one MBBA molecule was laid behind the L-0 ligand of a Δ-**Al-0** complex, then the second MBBA molecule was placed near the two acac ligands, and last the two octyloxy groups were introduced to generate Δ-**Al-2**. The search space may admittedly be biased by this procedure, and therefore, a number of different mutual orientations were considered later. A candidate for the stable structure was selected among the optimized structures from various initial states calculated at the HF level, which was then optimized further by density functional theory (DFT) calculations using the B3LYP functional in combination with the 3-21G** basis set. The lowest energy structure as far as we have examined is presented in Figure 4, while the configurations optimized at lower levels of calculation also involved twist angles (θ) within a range between −20° and −40°.

Acknowledgment. This work was supported in part by Grants-in-Aid for Scientific Research Nos. 13650941 and 15655016 from Ministry of Education, Culture, Sports, Science, and Technology (MEXT) of Japan. We thank Mr. Jun Yoshida for his assistance in the part of characterization, particularly for the NMR measurements, Ms. Seiko Oka and Ms. Miwa Kiuchi of Center for Instrumental Analysis, Hokkaido University, for the FAB-MS measurements, and Prof. Haruyuki Nakano of Department of Chemistry, Graduate School of Sciences, Kyushu University for his assistance in the computational part.

CM048121B

(32) Matsumura, K.; Iwayanagi, S. *Oyo Butsuri* (*J. Appl. Phys., Jpn.*) **1974**, *43*, 126−131.